JOURNAL OF THERMOPHYSICS AND HEAT TRANSFER
Vol. 17, No. 3, July–September 2003

Thermal Performance of a Triple-Glazed Exhausting and Ventilating Airflow Window System

Moo-Hyun Kim* and Chang-Yong Oh†
University of Ulsan, Ulsan 680-749, Republic of Korea
and
Wen-Jei Yang‡
University of Michigan, Ann Arbor, Michigan 48109-2125

The thermal performance and optimum design of a triple-glazed exhausting and ventilating airflow window system are studied numerically using a finite volume method. Exhausting and ventilating airflow rate, solar insolation, and aspect ratio are identified as important governing parameters. Effort is directed toward the reduction in space cooling and heating load. It is found that both space-heat gain and space-heat loss are reduced considerably by increasing the exhausting and ventilating airflow rate. The optimum airflow rate (Reynolds number) and aspect ratio are found to be about 600 and 0.05, respectively. Comparisons between the airflow window system and the enclosed window system are made qualitatively and quantitatively. The airflow window system with zero Reynolds number corresponds to the enclosed window case. The present airflow window model can be used year round, as an exhausting airflow type in summer and as a ventilating airflow type in winter.

Nomenclature

A	=	area of glazing, m^2
C	=	heat capacity, $kJ/m^3 \cdot K$
C_p	=	specific heat, $kJ/kg \cdot K$
c	=	clearance, m
Gr	=	Grashof number
g	=	gravitational acceleration, m/s^2
H	=	height of the window, m
h	=	convective heat transfer coefficient, $W/m^2 \cdot {}^\circ C$
I_t	=	solar insolation per unit area, W/m^2
k	=	thermal conductivity, $W/m \cdot K$
$\dot{m}$	=	air mass flowrate, kg/s
Ns	=	nondimensional number on heat absorption by panes
Nu	=	Nusselt number
$\boldsymbol{n}$	=	unit vector
P	=	pressure, kPa
Pe	=	Peclet number
Pr	=	Prandtl number
p	=	nondimensional pressure
q	=	absorbed energy per unit volume, W/m^3
Re	=	Reynolds number
S	=	width between panes, m
T	=	temperature, K
$T_{out,b}$	=	bulk temperature at the outlet, K
t	=	thickness of glazing, m
U, V	=	velocities of the x and y directions, m/s
u, v	=	dimensionless velocities of the x and y directions
V_∞	=	velocity of outdoor air, m/s
W	=	width of the window, m
X, Y	=	x and y coordinates, m
x, y	=	dimensionless x and y coordinates
α	=	thermal diffusivity, m^2/s
β	=	thermal expansion coefficient, 1/K
θ	=	dimensionless temperature
ν	=	kinematic viscosity, m^2/s
ρ	=	density, kg/m^3
σ	=	nondimensional clearance

Subscripts

f	=	fluid
o	=	outdoor
r	=	room/indoor
s	=	solid
1, 2, 3	=	outer, middle, inner pane
*	=	dimensionless value

Received 16 September 2002; revision received 30 November 2002; accepted for publication 2 December 2002.

*Professor, Department of Mechanical Engineering; mhkim@mail.ulsan.ac.kr.
†Graduate Student, Department of Mechanical Engineering.
‡Professor, Department of Mechanical Engineering; wjyang@engin.umich.edu.

Introduction

THE number of studies concerning energy-efficient building has considerably increased in recent years. It is commonly considered that windows are thermally most vulnerable parts in the building envelope, significantly contributing to increases in space heating as well as cooling load. Energy loss through windows amounts to over 3% of the total energy consumption in the United States.[1,2]

Research on thermal insulation problems of window systems has been actively conducted in many countries including the United States, Germany, Canada, and Finland. These window systems include, for example, those with closed space filled with noble gases such as argon, krypton, and xenon,[3,4] vacuum glazed windows,[2,5] and coated low-emissive glazed windows.[4,6] Unfortunately, these newly developed window systems are often expensive and uncomfortable for vision. The window systems in energy-efficient buildings, however, should have two important qualities: low energy loss and high residential comfort.

Airflow window systems often provide these two factors, as well as thermal comfort. In general, double-glazed windows have an enclosed air layer between two glasses, whereas airflow windows have an open-air layer between two pieces of glass or between a glass and a solid wall, through which diverse flow patterns can exist. Thus, the flow and thermal characteristics of airflow window systems are more complex in structures and difficult for fabrication. Airflow patterns between a glass and a roll screen were investigated to determine

thermal efficiency and effectiveness.[7] Many studies, mainly for applications to winter heating, of airflow types between a glass and a wall (passive trombe wall) were presented in Refs. 8 and 9. A study on a semi-open cavity with a screen and a siphon was conducted by Medved and Novak[10] to show how a screen provides good thermal insulation. There were numerous studies on double-glazed or double-pane window systems. However, few studies have been done on triple-glazed window systems. Theoretically, an enclosed triple-glazed window can reduce energy loss by about one-third more than an enclosed double-glazed window. Recently, Larsson et al.[11] investigated the thermal performance of an enclosed triple-glazed window system with low-emissivity coating and filled with krypton gas. Kim and Yang[12] studied the optimum design of a triple-glazed exhaust airflow window system for reducing the space cooling load in summer.

In this study, a numerical investigation is presented on a triple-glazed window with exhausting and/or ventilating airflow through open-air layers. In the exhausting airflow type, indoors air flows through the air layers and then exits outdoors. Air-mass flow rate carries the accumulated solar energy of the system out. Hence, this type is appropriate for reducing the space-cooling load in summer. In the ventilating airflow type, on the other hand, outdoors air flows through the air layers and then enters indoors. Air-mass flow rate carries the accumulated solar energy of the system in. Therefore, this type is suitable for reducing the space-heating load in winter. Three parameters, including the airflow rate, solar insolation, and aspect ratio, are selected to determine their roles on decrease in the space-heat gain and space-heat loss. Thermal performance and optimum values for design of the airflow window system are presented.

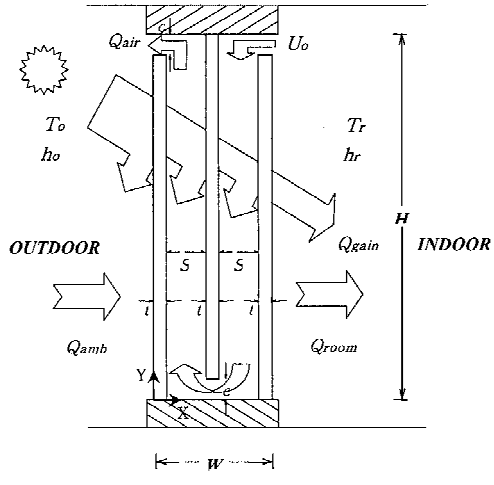

a) Exhausting airflow type

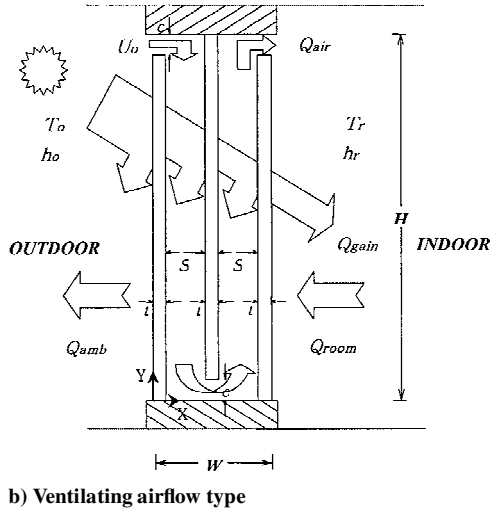

b) Ventilating airflow type

Fig. 1 Schematics of triple-glazed airflow windows.

Analytical Model

The triple-glazed airflow window systems to be studied are shown in Figs. 1a and 1b for an exhausting airflow type and a ventilating airflow type, respectively. The window systems are of height H and width W. The Cartesian coordinates with the corresponding velocity components u and v are indicated therein. Each system has two open-air spaces, the outer and the inner air spaces, and three glazings, the outer, the middle and the inner glazings. In the exhausting type, indoors air enters through the inlet clearance at the top of the inner glazing and exits through the outlet clearance. In the ventilating type, outdoors air enters through the inlet clearance at the top of the outer glazing and exits through the outlet clearance at the top of the inner glazing.

This study treats the problems of mixed convections induced by a combination of the buoyancy effect and the forced inlet/outlet flows by fan. The physical model for the numerical calculation does not take any frame into consideration, that is, only the air spaces and solid glasses are calculated. The computational domain includes both fluid and solid layers, thus, formulating a conjugate problem. In this study, glazing is assumed to be a heat source that absorbs a portion of solar energy and then emits part of that energy, and radiation effect between glazings is not included.

Mathematical Formulation

The flow is assumed to be steady, laminar, incompressible, and two-dimensional. Viscous dissipation is neglected, and properties of the fluid are assumed to be constant except for the buoyancy term in the y-momentum equation, that is, the Boussinesq approximation. The equations are obtained in dimensionless forms as follows:

$$\frac{\partial u}{\partial x}+\frac{\partial v}{\partial y}=0 \tag{1}$$

$$u\frac{\partial u}{\partial x}+v\frac{\partial u}{\partial y}=-\frac{\partial p}{\partial x}+\frac{\nu^*\sigma}{Re}\left(\frac{\partial^2 u}{\partial x^2}+\frac{\partial^2 u}{\partial y^2}\right) \tag{2}$$

$$u\frac{\partial v}{\partial x}+v\frac{\partial v}{\partial y}=-\frac{\partial p}{\partial y}+\frac{\nu^*\sigma}{Re}\left(\frac{\partial^2 v}{\partial x^2}+\frac{\partial^2 v}{\partial y^2}\right)+\frac{Gr\sigma^2}{Re^2}\theta[1-f(\Omega)] \tag{3}$$

$$u\frac{\partial \theta}{\partial x}+v\frac{\partial \theta}{\partial y}=\frac{k^*\sigma}{PeC^*}\left(\frac{\partial^2 \theta}{\partial x^2}+\frac{\partial^2 \theta}{\partial y^2}\right)+\frac{Ns\sigma}{PeC^*}f(\Omega) \tag{4}$$

These equations were nondimensionalized using the following nondimensional variables:

$$x=\frac{X}{H},\qquad y=\frac{Y}{H},\qquad u=\frac{U}{U_o},\qquad v=\frac{V}{U_o}$$

$$p=\frac{P}{\rho U_o^2},\qquad \theta=\frac{T-T_r}{T_o-T_r},\qquad Re=U_o\frac{(2c)}{\nu_f}$$

$$Pr=\frac{\nu_f}{\alpha_f},\qquad Gr=\frac{g\beta(T_o-T_r)H^3}{\nu_f^2},\qquad Pe=Re\cdot Pr$$

$$Ns=\frac{q\cdot H^2}{k_f(T_o-T_r)},\qquad \sigma=\frac{2c}{H},\qquad k^*=\frac{k}{k_f}$$

$$C^*=\frac{(\rho C_p)}{(\rho C_p)_f},\qquad \nu^*=\frac{\nu}{\nu_f} \tag{5}$$

where ν^*, k^*, and C^* are the dimensionless kinematic viscosity, thermal conductivity, and thermal capacitance, respectively. All variables are unity in the fluid region. In the solid region, however, $\nu=\nu_s$, $k=k_s$, $(\rho C_p)=(\rho C_p)_s$, and the dimensionless kinematic viscosity $\nu^*(=\nu_s/\nu_f)$ is on the order of 10^5 or 10^6, large enough to be treated as solid in numerical calculations. Here $f(\Omega)$ is a step function that is equal to zero in the fluid region (air spaces) and

unity in the solid region (panes). In this mixed convective calculation, Reynolds number covers the range of $0 \sim 1500$ and Grashof number is 1.05×10^9 in the exhausting case and 2.71×10^9 in the ventilating case.

The appropriate hydrodynamic, thermal, and solid–fluid interfacial boundary conditions are specified as follows.

The velocity boundary conditions at $Y = 0, H$ are

$$u = 0, \qquad v = 0 \tag{6a}$$

at pane surfaces are

$$u = 0, \qquad v = 0 \tag{6b}$$

and at air inlet clearance in the exhausting and in the ventilating airflow types are, respectively,

$$u = -1 \tag{6c}$$

$$u = 1 \tag{6d}$$

The thermal boundary conditions at $Y = 0, H$ are

$$\frac{\partial \theta}{\partial y} = 0 \tag{7a}$$

at $X = W$ are

$$\frac{Nu_r}{k^*}\theta_s = -\frac{\partial \theta_s}{\partial x} \tag{7b}$$

at $X = 0$ are

$$\frac{Nu_o}{k^*}(\theta_s - 1) = \frac{\partial \theta_s}{\partial x} \tag{7c}$$

and at air inlet clearance in the exhausting and in the ventilating airflow types are, respectively,

$$\theta = 0 \tag{7d}$$

$$\theta = 1 \tag{7e}$$

Nu_r and Nu_o are the Nusselt numbers calculated at the inside surface of the inner pane and at the outside surface of the outer pane, respectively. They are defined as

$$Nu_r = h_r H/k_f, \qquad Nu_o = h_o H/k_f \tag{8}$$

The fluid–solid interfacial conditions are

$$\theta_f = \theta_s, \qquad k_f \frac{\partial \theta_f}{\partial \boldsymbol{n}} = k_s \frac{\partial \theta_s}{\partial \boldsymbol{n}} \tag{9}$$

where $\boldsymbol{n}$ is a unit vector at the solid–fluid interface.

An energy balance for the control volume of window system is obtained as

$$Q_{\text{gain}} + Q_{\text{amb}} + Q_{\text{room}} + Q_{\text{air}} = 0 \tag{10}$$

where Q_{gain} is the portion of solar energy absorbed by the panes, Q_{amb} the efflux energy transferred outdoors through the outer pane, Q_{room} the influx energy transferred indoors through the inner pane, and Q_{air} the energy transported by air-mass flow rate. Q_{room} is the energy of the room- or space-heat gain through the inner pane, which results in an increase in space cooling load in summer. Equation (10) can be rewritten as

$$(Q_{\text{amb}} + Q_{\text{room}} + Q_{\text{air}})/Q_{\text{gain}} = -1 \tag{11}$$

Equation (11) is used to validate the analytical model and its computation presented here. Each term in Eq. (10) may be expressed as

$$Q_{\text{gain}} = (q_1 + q_2 + q_3)At, \qquad Q_{\text{amb}} = h_o A(T_o - T|_{x=0})$$

$$Q_{\text{room}} = h_r, A(T_r - T|_{x=w}), \qquad Q_{\text{air}} = \dot{m} C_p (T_r - T_{\text{out,b}}) \tag{12}$$

Table 1 Properties of glass and air

Property	Glass	Air
Conductivity k, W/m · K	0.756	0.025
Density ρ, kg/m^3	2550	1.165
Specific heat C_p, J/kg · K	754	1006
Kinematic viscosity ν, m^2/s	——	1.5×10^{-5}
Prandl number Pr	——	0.70
Absorptivity	0.139	——
Reflectivity	0.072	——
Transmissivity	0.789	——

Table 2 Specifications of triple-glazed airflow window systems in meters

Aspect ratio, W/H	Width, W	Height, H	Thickness, t	Clearance, c	Width, S
0.03	0.027	0.900	0.006	0.005	0.0045
0.04	0.036	0.900	0.006	0.005	0.0090
0.05	0.045	0.900	0.006	0.005	0.0135
0.10	0.090	0.900	0.006	0.005	0.0360

Here, q_1, q_2, and q_3 are the heats absorbed per unit volume by the three panes 1, 2, and 3 and can be expressed as

$$q_1 = (I_t/t) \cdot A_{3(1)}, \qquad q_2 = (I_t/t) \cdot A_{3(2)}, \qquad q_3 = (I_t/t) \cdot A_{3(3)} \tag{13}$$

$A_{3(1)}$, $A_{3(2)}$, and $A_{3(3)}$ are the absorptivities of the outer, middle, and inner panes, respectively, to be determined using the net radiation method.[13] The external convective heat transfer coefficient h_o, in watts per square meter degrees Celsius, and the internal convective heat transfer coefficient h_r, in watts per square meter degrees Celsius, are calculated from the relationships suggested by McAdams[14] as

$$h_o = 8.07V^{0.605}, \qquad V_\infty > 2.0$$

$$h_r = 1.42(\Delta T/H)^{\frac{1}{4}} \tag{14}$$

In the case of the ventilating airflow type, the outdoors temperature T_o is used instead of T_r for the calculation of Q_{air} in Eq. (12). In the present study, $T_r = 24^\circ$C and $T_o = 35^\circ$C are employed for the exhausting airflow type in summer and $T_r = 22^\circ$C and $T_o = -1.2^\circ$C for the ventilating airflow type in winter.

The governing equations are solved using the finite volume method developed by Patankar.[15] A grid system of 40×110 nodes is used in basic calculation. The solution domain is discretized using a nonuniform mesh with smaller grid spacing near the glazings and larger spacing in the interior. Results obtained with finer grids did not show any noticeable changes in the flowfield and calculated heat rates. The relaxation factors are 0.7, 0.3, and 0.4 for the energy equation, momentum equation, and pressure-correction equation, respectively. The number of iterations is approximately 1500–4000, and the criterion for numerical convergence that is, the maximum relative difference between two consecutive iterations, is less than 10^{-6}. The properties of the air and glass and the specifications of the window system are listed in Tables 1 and 2, respectively.

Results and Discussions

Figure 2 shows the calculated energies, Q/Q_{gain} in dimensionless form against the Reynolds number Re. Results provide an insight into the energy balance characteristics of the system with increasing Reynolds number. The Reynolds number implies the flow rate of exhaust air through the air spaces. $Re = 0$ corresponds to the case of enclosed windows. The minus sign (−) indicates the energy efflux from the control volume to the surrounding area, whereas plus sign (+) indicates the energy influx from the surrounding area to the control volume.

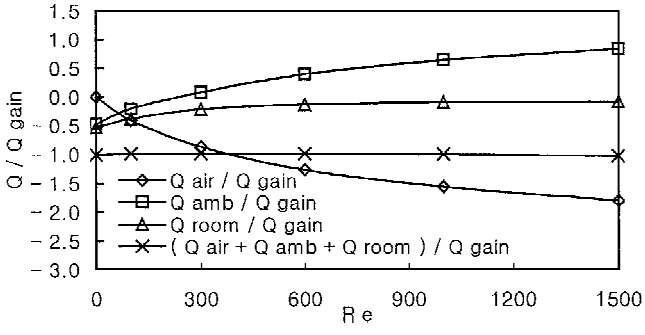

Fig. 2 Calculated heat rates for the exhausting airflow type at $I_t = 100$ W/m^2.

Observe in Fig. 2 that the magnitude (absolute value) of Q_{air}/Q_{gain} grows with an increase in Reynolds number Re, which implies that energy loss to the surroundings by convection increases with Reynolds number Re. The room-heat gain (or space-heat gain), Q_{room}/Q_{gain}, however, diminishes and approaches zero as the Reynolds number increases. Note that, in summer, the space-heat gain can be reduced considerably by increasing the exhaust airflow rate. Discussion of the optimum exhaust airflow rate will be presented later. The energy transfered outdoors, Q_{amb}/Q_{gain}, shows both heat efflux through the outer pane at $Re = 0$ and heat influx through the outer pane at $Re \geq 200$.

Figure 3 shows the global views of the streamline and isotherm for the exhausting, ventilating, and enclosed airflow windows to aid in investigating the effects of solar insolation on the flow and temperature fields. In the case of the exhausting window at $Re = 300$, Fig. 3a shows a clockwise cell at both the lower part of the outer air space and the upper part of the inner air space. As the solar insolation I_t increases, the intensity of the cell at the upper part of the inner air space increases due to an increase in the buoyancy effect. In contrast, in the case of the ventilating window at $Re = 300$, Fig. 3b shows a counterclockwise cell at both the upper part of the outer air space and the lower part of the inner air space. As the solar insolation increases, the intensity of the cell at the upper part of the outer air space increases due to an increase in the buoyancy effect. However, the flow and thermal characteristics of the airflow systems are different from those of the enclosed system as given in Fig. 3c. In the case of the enclosed system in summer at $Re = 0$, two cells in the outer air layer and unicell in the inner air layer appear at $I_t = 100$ W/m^2. As the solar intensity is increased to 400 and 600 W/m^2, a unicell appears in each air layer. Note that the unicell in the outer layer rotates counterclockwise, whereas the unicell in the inner layer revolves clockwise because the temperature of middle pane is higher than those of the other panes, as shown in Fig. 4.

It seems that the airflow rate through the air spaces is the most important variable in the present parametric study. In the case of the exhausting airflow type, Figure 5a plots the room/space-heat gain $-Q_{room}$ vs the Reynolds number at $I_t = 600$ W/m^2. Observe that the space-heat gain is substantially reduced with an increase in Reynolds numbers, that is, the exhausting airflow rate.

At $Re = 0$, in the absence of exhausting airflow, the space-heat gains take a value of about 72 ~ 75 W for four aspect ratios. The space-heat gain, however, decreases almost exponentially as the Reynolds number increases. The decrements in the space-heat gains are considerably larger in the range of low Reynolds numbers and level off in the range of $Re \geq 600$. Evidently, the optimum value of the exhausting airflow rate must be around of $Re = 600$. Under the optimum conditions, the space-heat gain is approximately 30 W, corresponding to 40% of that of the enclosed window. It implies a 60% decrease compared to the enclosed windows. In the case of the ventilating airflow type, Fig. 5b shows that the space-heat loss $-Q_{amb}$ also decreases almost exponentially as the airflow rate increases. The space-heat losses take a value of approximately 150 W for all aspect ratios at $Re = 0$ for no ventilating airflow. At $Re = 600$ and $W/H = 0.05$, the space-heat loss is about 80 W, which corresponds to 53% of the enclosed window case.

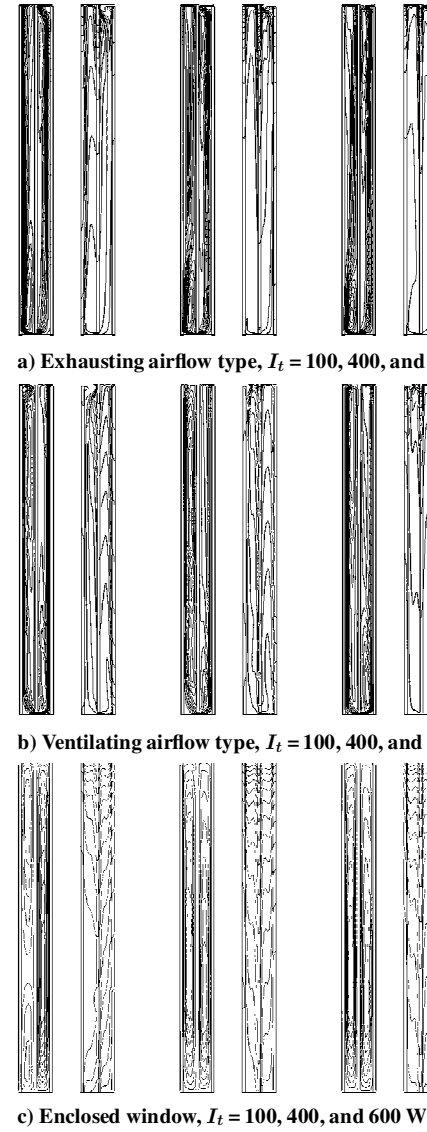

a) Exhausting airflow type, $I_t = 100$, 400, and 600 W/m^2

b) Ventilating airflow type, $I_t = 100$, 400, and 600 W/m

c) Enclosed window, $I_t = 100$, 400, and 600 W/m

Fig. 3 Effects of solar insolation on streamlines and isotherms at $W/H = 0.1$ and $Re = 300$.

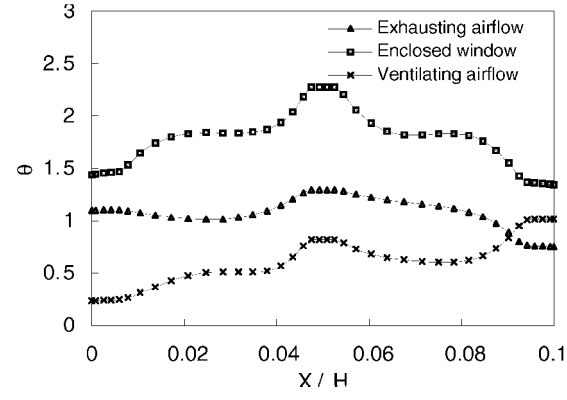

Fig. 4 Temperature profile at midheight ($H/2$) for $W/H = 0.1$, $Re = 300$, and $I_t = 400$ W/m^2.

A change in the aspect ratio W/H results in changes in both the space-heat gain and the space-heat loss under identical physical situation. Numerical results for four aspect ratios at $I_t = 100$ W/m^2 are presented in Fig. 5. It is seen in Fig. 6a and 6b that the effects of the aspect ratio on both the space-heat gain and the space-heat loss are negligible in the range of $Re > 600$. However, it becomes important in the range of $Re \leq 600$. In the range of small Reynolds numbers, lower than $Re = 300$, reductions in both space-heat gain

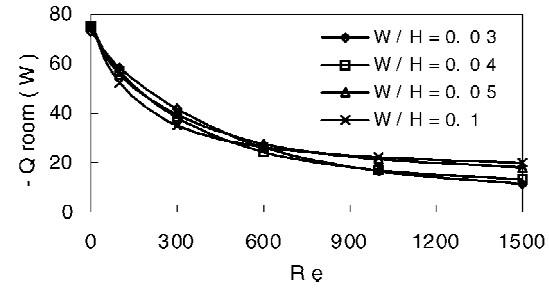

a) Exhausting airflow type

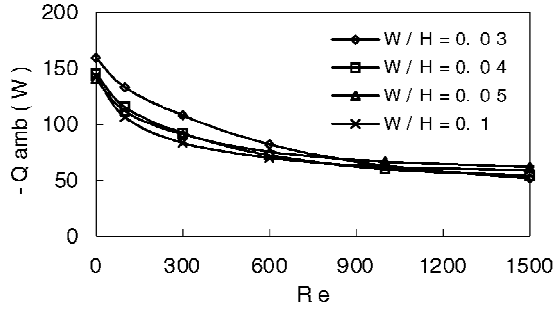

b) Ventilating airflow type

Fig. 5 Effect of airflow rate on the space-heat gain and the space-heat loss at $I_t = 600$ W/m^2.

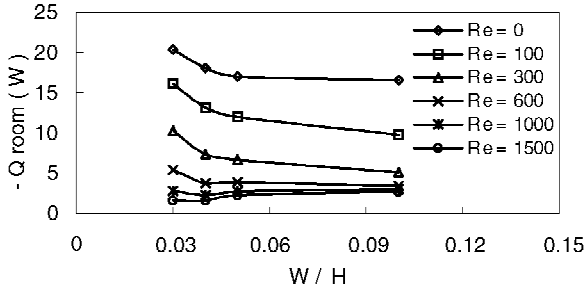

a) Exhausting airflow type

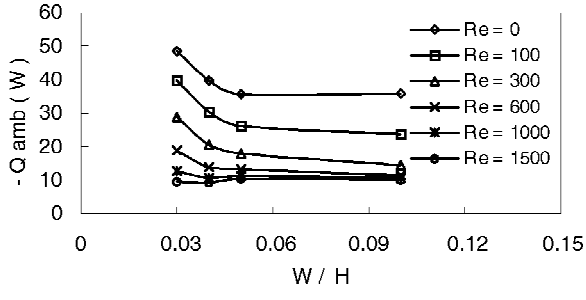

b) Ventilating airflow type

Fig. 6 Effect of aspect ratio on the space-heat gain and the space-heat loss at $I_t = 100$ W/m^2.

and space-heat loss become significant with a change in the aspect ratio, especially for $W/H \leq 0.05$. This suggests that the value of the aspect ratio W/H around 0.05 is suitable for the optimum value in the present numerical analysis.

Conclusions

The thermal performance and optimum design of airflow window systems to provide low energy loss and high thermal comfort have been studied numerically. A triple-glazed airflow window model has been selected for a parametrical study to determine the effects of solar insolation, exhausting and ventilating airflow rate, and aspect ratio on reduction in the space-heat gain and space-heat loss, which represent decline in the space cooling load and space heating load through windows. The results obtained have been compared with those of an enclosed window system.

For the exhausting airflow window, clockwise cells have been observed in the air spaces. For the ventilating airflow window, however, counterclockwise cells appear in the air spaces. When solar insolation is increased, the intensity of the cell formed at the upper part of the air space increases due to an enhancement in the buoyancy effect. Both space-heat gain and space-heat loss decrease almost exponentially as the exhausting and ventilating airflow rates are increased. The decrements in the space-heat gain and space-heat loss are considerably higher in low Reynolds number range, but are relatively low in the range of $Re \geq 600$. The optimum airflow rate and aspect ratio have been found to be about $Re = 600$ and 0.05, respectively. Under the optimum condition, the space-heat gain and space-heat loss through the window systems would achieve a 60% decrease of that for enclosed windows. It is concluded that the proposed airflow window model is applicable year round, the exhausting airflow type for use in summer and the ventilating airflow type in winter.

Acknowledgment

This work was supported by the University of Ulsan Research Fund of 2002 in Ulsan, Republic of Korea.

References

[1]Arasteh, D., Selkowitz, S., and Wolfe, J. R., "The Design and Testing of a Highly Insulating Glazing System for Use with Conventional Window Systems," *Journal of Solar Energy Engineering*, Vol. 111, No. 3, 1989, pp. 44–53.

[2]Collins, R. E., Turner, G. M., Fisch-Cripps, A. E., and Tang, J. Z., "Vacuum Glazing—A New Component for Insulating Windows," *Building and Environment*, Vol. 30, No. 4, 1995, pp. 459–492.

[3]Hanley, H. J. M., McCarty, R. D., and Haynes, W. M., "The Viscosity and Thermal Conductivity Coefficients for Dense Gaseous and Liquid Argon, Krypton, Xenon, Nitrogen and Oxygen," *Journal of Physical and Chemical Reference Data*, Vol. 3, No. 4, 1974, pp. 979–1018.

[4]Weir, G., and Muneer, T., "Energy and Environmental Impact Analysis of Double-Glazed Windows," *Energy Conversion and Management*, Vol. 39, No. 3–4, 1998, pp. 243–256.

[5]Collins, R. E., Davis, C. A., Dey, C. J., Robinson, S. J., Tang, J. Z., and Turner, G. M., "Measurement of Local Heat Flow in Flat Evacuated Glazing," *International Journal of Heat and Mass Transfer*, Vol. 36, No. 10, 1993, pp. 2550–2563.

[6]Granqvist, C. G., "Energy Efficient Windows: Present and Forthcoming Technology," *Materials Science for Solar Energy Conversion Systems*, Pergamon, Oxford, 1991, p. 106.

[7]Tanimoto, J., and Kimura, K., "Simulation Study on an Air Flow Window System with an Integrated Roll Screen," *Energy and Buildings*, Vol. 26, No. 3, 1997, pp. 317–325.

[8]Barozzi, G. S., Ibabi, M. S. E., Nobile, E., and Sousa, A. C. M., "Physical and Numerical Modeling of a Solar Chimney-Based Ventilation System for Building," *Building and Environment*, Vol. 27, No. 4, 1992, pp. 433–441.

[9]Gan, G., "A Parametric Study of Trombe Walls for Passive Cooling of Buildings," *Energy and Buildings*, Vol. 27, No. 1, 1998, pp. 37–43.

[10]Medved, S., and Novak, P., "Heat Transfer Through a Double Pane Window with an Insulation Screen Open at the Top," *Energy and Buildings*, Vol. 28, No. 3, 1998, pp. 257–268.

[11]Larsson, U., Moshfegh, B., and Snadberg, M., "Thermal Analysis of Super Insulated Windows (Numerical and Experimental Investigations)," *Energy and Buildings*, Vol. 29, No. 2, 1999, pp. 121–128.

[12]Kim, M.-H., and Yang, W.-J., "An Optimum Design on the Triple-Glazed Exhaust Airflow Window," *International Journal of Energy Research*, Vol. 26, No. 4, 2002, pp. 355–364.

[13]Siegel, R., and Howell, J. R., *Thermal Radiation Heat Transfer*, McGraw–Hill, New York, 1972, pp. 235–250.

[14]McAdams, W. H., *Heat Transmission*, 3rd ed., McGraw–Hill, New York, 1954, Chap. 7.

[15]Patankar, S. V., *Numerical Heat Transfer and Fluid Flow*, McGraw–Hill, New York, 1980, Chaps. 5, 6.